MEMORANDUM
RM-4483-PR
MARCH 1965

HYPERSONIC TURNING WITH CONSTANT BANK ANGLE CONTROL

F. S. Nyland

PREPARED FOR:
UNITED STATES AIR FORCE PROJECT RAND

The RAND Corporation
SANTA MONICA • CALIFORNIA

MEMORANDUM
RM-4483-PR
MARCH 1965

HYPERSONIC TURNING WITH CONSTANT BANK ANGLE CONTROL

F. S. Nyland

This research is sponsored by the United States Air Force under Project RAND—Contract No. AF 49(638)-700 monitored by the Directorate of Development Plans, Deputy Chief of Staff, Research and Development, Hq USAF. Views or conclusions contained in this Memorandum should not be interpreted as representing the official opinion or policy of the United States Air Force.

The RAND Corporation
1700 MAIN ST • SANTA MONICA • CALIFORNIA • 90406

Published by The RAND Corporation

PREFACE

This Memorandum is the result of further study of the trajectories of glide reentry vehicles. Related Memoranda, which were based on previous investigations of the use of the atmospheric forces to effect changes in the orbital plane for winged spacecraft, include RM-4391-PR, Minimum Energy Loss Heading Changes for Hypersonic Flight from Orbit, by Russell D. Shaver and RM-3231-PR, The Synergetic Plane Change for Orbiting Spacecraft, by F. S. Nyland.

This present study is part of several continuing analyses related to space operations. It should be of interest to planners, analysts in the fields of atmospheric reentry, designers of advanced space vehicles, and persons concerned with maneuvering space vehicles and their utility.

SUMMARY

This Memorandum presents the elements of a model for predicting the turning trajectories of hypersonic reentry gliders by approximate closed form solutions. Vehicle control is assumed to be exercised by varying the angle of attack and bank angle. In this investigation the control variables are assumed to be constant for each particular trajectory, but the lift-to-drag ratio (L/D) has been varied from 1.0 to 4.0 and the bank angle has been permitted to become as large as 90 deg. Approximate closed form solutions are compared with earlier results of a study of minimum energy hypersonic turns.

CONTENTS

PREFACE iii

SUMMARY v

SYMBOLS ix

Section

I. INTRODUCTION 1

II. EQUATIONS OF MOTION 3

III. TRAJECTORIES FOR BANK ANGLES LESS THAN 90 DEGREES 6

IV. TRAJECTORIES FOR BANK ANGLES OF 90 DEGREES 22

V. HEATING TRENDS 35

VI. FINAL COMMENTS 37

REFERENCES 43

SYMBOLS

$a = \dfrac{2}{(L/D) \sin \phi}$

A = aerodynamic reference area

$b = \dfrac{g \rho_o C_D A}{2 \beta W \sin (-\gamma)}$

C_D = drag coefficient

C_L = lift coefficient

D = drag force

g = acceleration due to gravity

h = altitude

L = lift force

n = integer

R_o = earth radius (3442 n mi)

s = path length

t = time

u = vehicle velocity

u_f = final velocity

u_i = initial velocity

u_o = satellite velocity at 200,000 ft (25,815 ft/sec)

u_r = reentry velocity

W = vehicle weight

x = downrange distance

y = siderange distance

$z = \log_e (u/u_r)^{L/D}$ = a dummy variable

β = inverse of atmospheric scale height (1/24,000 ft)

γ = flight path angle (measured positive upwards)

σ = $e^{-\beta h}$ = density factor

ρ_o = sea level density of air (0.07648/32.2 slugs/ft^3)

ϕ = bank angle

ω = heading angle

I. INTRODUCTION

In past studies, several authors have presented closed form solutions to describe the turning trajectories of lifting vehicles entering the atmosphere.[1, 2, 3] Loh achieved approximate closed form solutions by specifying the shape of the ground track, a minor circle. Slye showed approximate solutions for constant bank angle control of vehicles with low lift-to-drag ratios ($0 < L/D < 2$), but his main emphasis was on maximizing the side range, rather than minimizing energy loss for a given heading change. In this Memorandum, approximate closed form solutions will be developed that may be applied to a greater range of lift-to-drag ratios where the vehicle bank angles of interest will be particularly steep, even up to 90 deg. The approach here is quite similar to the one used by Slye, but it additionally considers near-ballistic reentries in which all lift is used to change the vehicle heading.

The interest in constant bank angle control is basically twofold. Such a control law is easy to mechanize by either automatic or pilot control. Secondly, a recent investigation of turning trajectories by Shaver [4] showed that such a control law may be nearly optimal for synergetic plane changing[5] where the optimal path is defined as that trajectory which minimizes the energy loss during the aerodynamic portion of flight for a given vehicle heading change. Shaver's work also indicates that the optimal control law for the angle of attack is for the vehicle to fly at an attitude that results in the maximum lift-to-drag ratio. Thus, as a result of this recent work, the problem is no longer determining optimal control laws, but rather

finding a simple way of describing flight trajectories that minimize energy losses. This Memorandum derives the descriptive material necessary for making preliminary determinations of the trajectory shapes. A constant bank angle control scheme that assumes a constant lift-to-drag ratio is used.

In addition to synergetic plane changing, there are other applications. There has always been an interest in the side range that a reentering vehicle can achieve, and such calculations will be presented later in this Memorandum.

II. EQUATIONS OF MOTION

The equations of motion used in this analysis have been written as a resolution of accelerating influences along the flight path, along a line perpendicular to the flight path in a generally up and down direction, and in a direction out of the flight plane. The accelerations in these various directions are assumed to be controllable by a variation in the bank angle and the lift-to-drag ratio. These equations also include the assumption that the acceleration due to gravity does not change very much in the altitude regime of interest. Therefore, the orbital velocity may be written as $u_o^2 = R_o g$, where R_o is the sum of the earth's radius and reference altitude, and g is the acceleration due to gravity at the reference altitude.

The accelerations along the flight path may be expressed as

$$\frac{1}{g}\frac{du}{dt} = -\sin\gamma - \frac{D}{W} = \frac{1}{2g}\frac{du^2}{ds} \qquad (1)$$

where u is the vehicle speed, t is time, γ is the flight path angle in the vertical direction, D is the drag force, and W is the vehicle weight. Fig. 1 shows the flight geometry.

Along the local vertical,

$$\frac{u}{g}\frac{d\gamma}{dt} = \frac{L}{W}\cos\phi - (1 - u^2/u_o^2)\cos\gamma \qquad (2)$$

where L is the lift force, ϕ is the bank angle, and u_o is the orbit speed at a reference altitude of 200,000 ft.

Crossways to the flight path, the heading change with time is

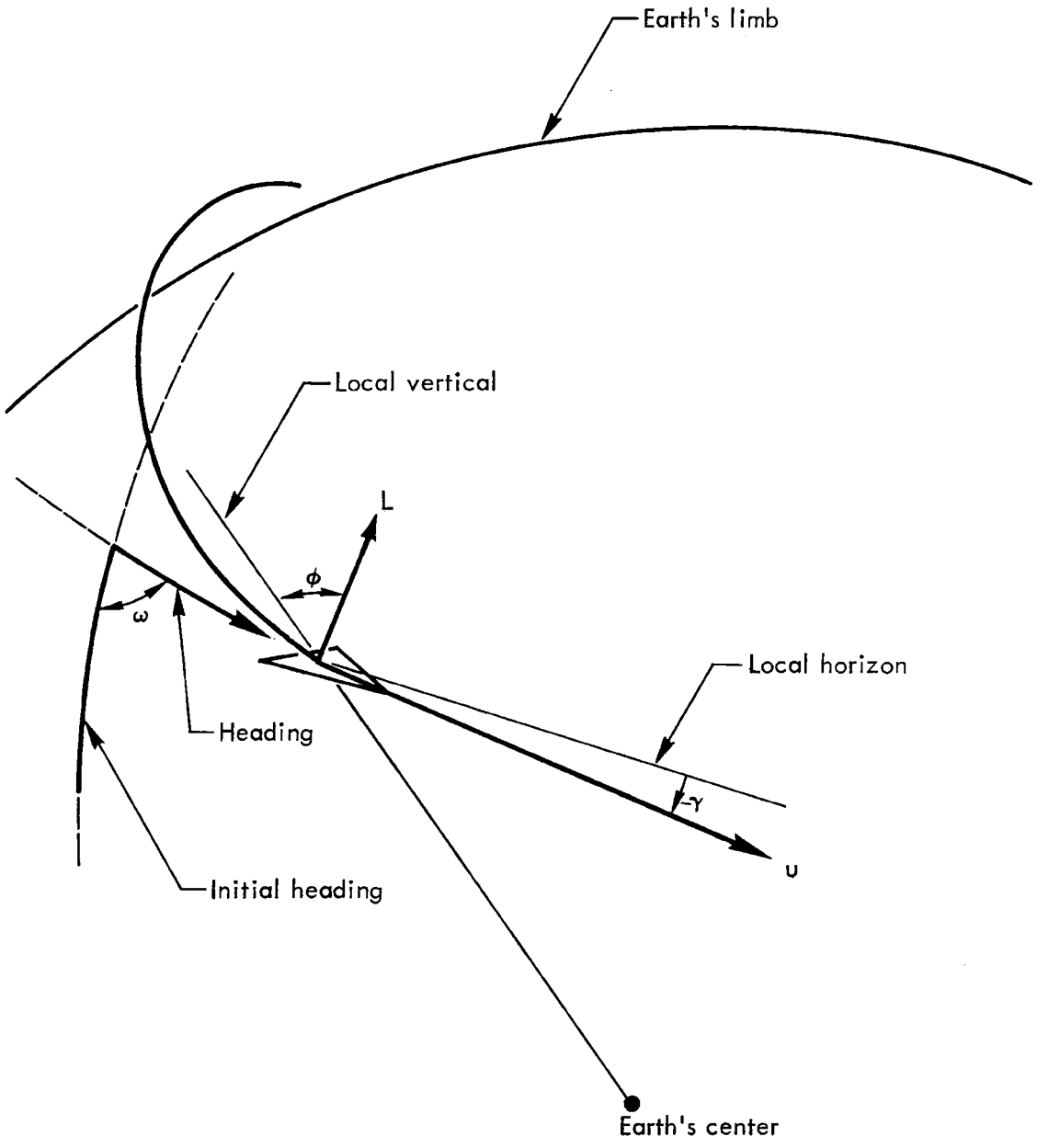

Fig. 1—Flight trajectory coordinates

$$\frac{u}{g}\frac{d\omega}{dt} = \frac{L}{W}\sin\phi \qquad (3)$$

where ω is the flight path angle sideways (heading angle) of the vehicle. Equation 3 is a balance of forces in the plane established by the center of curvature and two points very close to each other on the trajectory, but does not include the higher order terms introduced by the earth's curvature.

III. TRAJECTORIES FOR BANK ANGLES LESS THAN 90 DEGREES

In this section, solutions to the equations of motion will be found for turning trajectories where the bank angle is less than 90 deg. Whenever possible, closed form solutions will be sought if only minor errors are committed in making approximations. For one part of the following trajectory description, such a solution is apparently not possible; the results of numerical integration will be presented for a large range of parameter variations.

Our assumptions are quite similar to those commonly used in analyses of lifting trajectories. It is assumed that:

1) the flight path angle (hereafter referring only to the up and down direction) is very small
2) the acceleration due to gravity changes only slightly in the regions of interest, and that such changes may be neglected
3) the predominant deceleration influence is due to drag
4) the flight path angle does not vary greatly ($d\gamma/dt \cong 0$)
5) the control variables, L/D and ϕ, are constant throughout the flight regime.

These assumptions appear to introduce only small errors in the solutions to the equations of motion provided there is some component of lift along the local vertical, so that the path angle can be reasonably maintained at small values ($\gamma \ll D/W$). For the particular case in which there is no component of lift along the local vertical, one must make other assumptions to find closed form solutions. Thus, a later part of this Memorandum will be devoted to solving the equations of motion when

the bank angle is 90 deg and there is no component of lift along the local vertical.

Under these assumptions, the equations of motion become

$$\frac{1}{g}\frac{du}{dt} = -\frac{D}{W} = \frac{1}{2g}\frac{du^2}{ds} \tag{1a}$$

$$\frac{L}{W}\cos\phi = 1 - u^2/u_o^2 \tag{2a}$$

$$\frac{u}{g}\frac{d\omega}{dt} = \frac{L}{W}\sin\phi \tag{3a}$$

Combining equations 1a and 3a to eliminate time as a variable and integrating from an initial velocity where the turn is started,

$$\omega = \frac{L}{D}\sin\phi \log_e (u_i/u) \tag{4}$$

This result indicates that the turning rate is highest at the end of a turn or that the turning rate increases as the vehicle slows down (Fig. 2). The largest heading changes can be accomplished with maximum L/D and very steep bank angles. From equation 2a, the normal load factor also increases as the vehicle slows down. These trends are the same as those noted by Shaver in optimizing synergetic plane changes.[4]

To determine the altitude-velocity profile, the lift force may be rewritten as

$$L = \frac{1}{2}\rho_o e^{-\beta h} u^2 C_L A$$

where ρ_o is the sea level air density (slugs/ft^3), β is the inverse of scale height of the atmosphere, h is the altitude, C_L is the lift

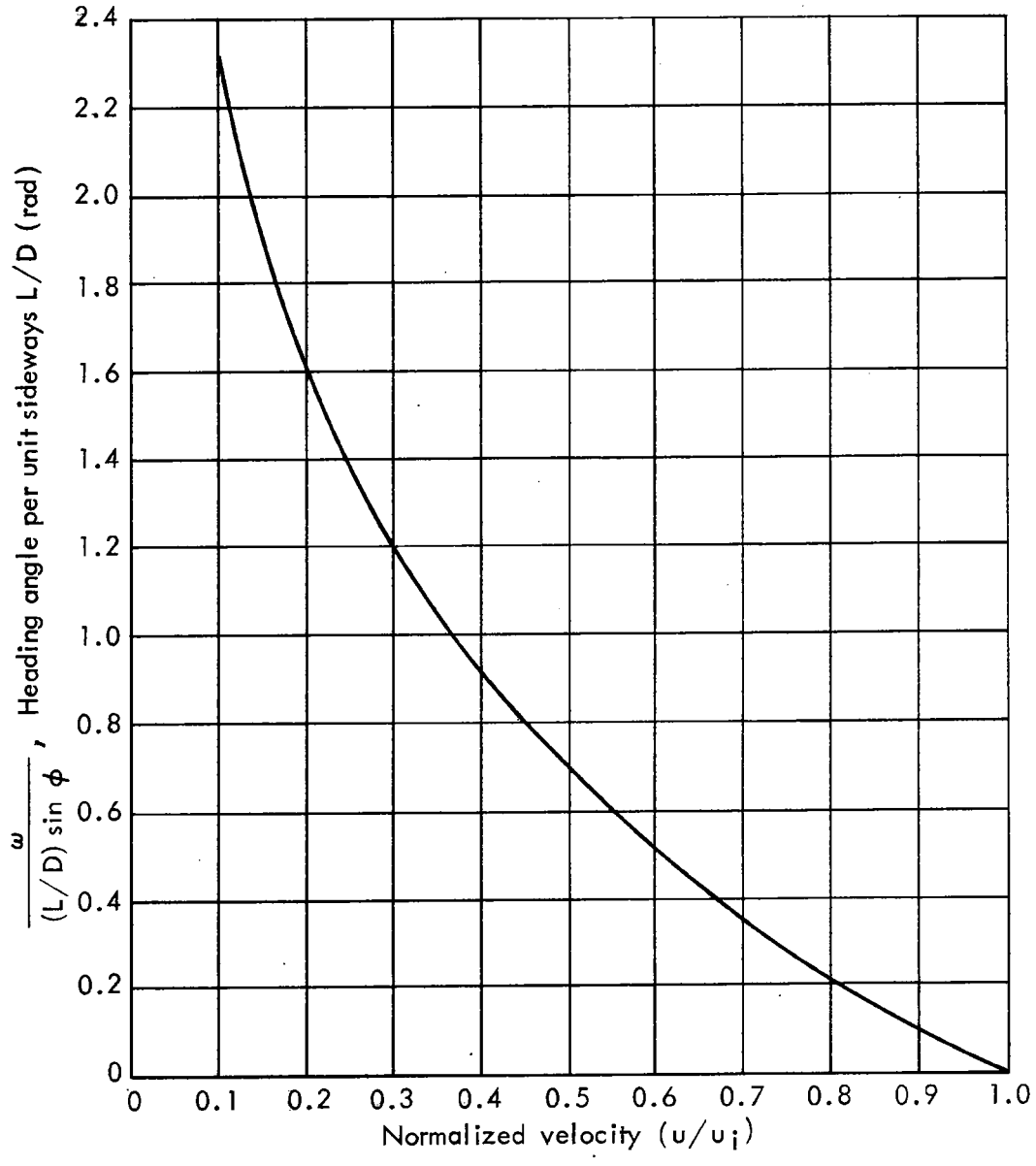

Fig. 2—Heading angle-velocity relation

coefficient, and A is the vehicle reference area. Substituting this statement into equation 2a, then

$$e^{\beta h} = \left(\frac{1}{2} u_o^2 \rho_o\right) \left(\frac{u^2/u_o^2}{1 - u^2/u_o^2}\right) \left(\frac{C_L A}{W}\right) \cos \phi$$

Solving for βh, and separating into convenient quantities, note that

$$\beta h = \log_e \frac{1}{2} u_o^2 \rho_o - \log_e (u_o^2/u^2 - 1) - \log_e \frac{W}{C_L A} - \log_e (1/\cos \phi) \qquad (5)$$

From this result it is possible to construct a simple calculating tool that can be used to find the altitude-velocity profile for constant bank angle control routines (Fig. 3). This figure shows contours for various bank angles with the lift parameter, $W/C_L A$, set to unity. For other values of $W/C_L A$, a scale is given that shows the altitude decrement for variations in this parameter. Also shown are flat plate temperatures to indicate the heating trend, should this be of interest.[6] Note here that because the fundamental shape of the equilibrium glide profile is unchanged by variations in the bank angle, the maximum heating rate for constant bank angle trajectories appears to be less than for minor circle turn trajectories. Minor circle profiles are such that the vehicle will be at lower altitudes than would be the case for a constant bank angle contour at the same velocity in the high velocity regime where the maximum heating rate occurs. This assumes that the $W/C_L A$ is the same in each case. Also, the velocity of maximum heating rate is shifted to higher values for the minor circle turn.[1] Such is not the case for constant bank angle control, and

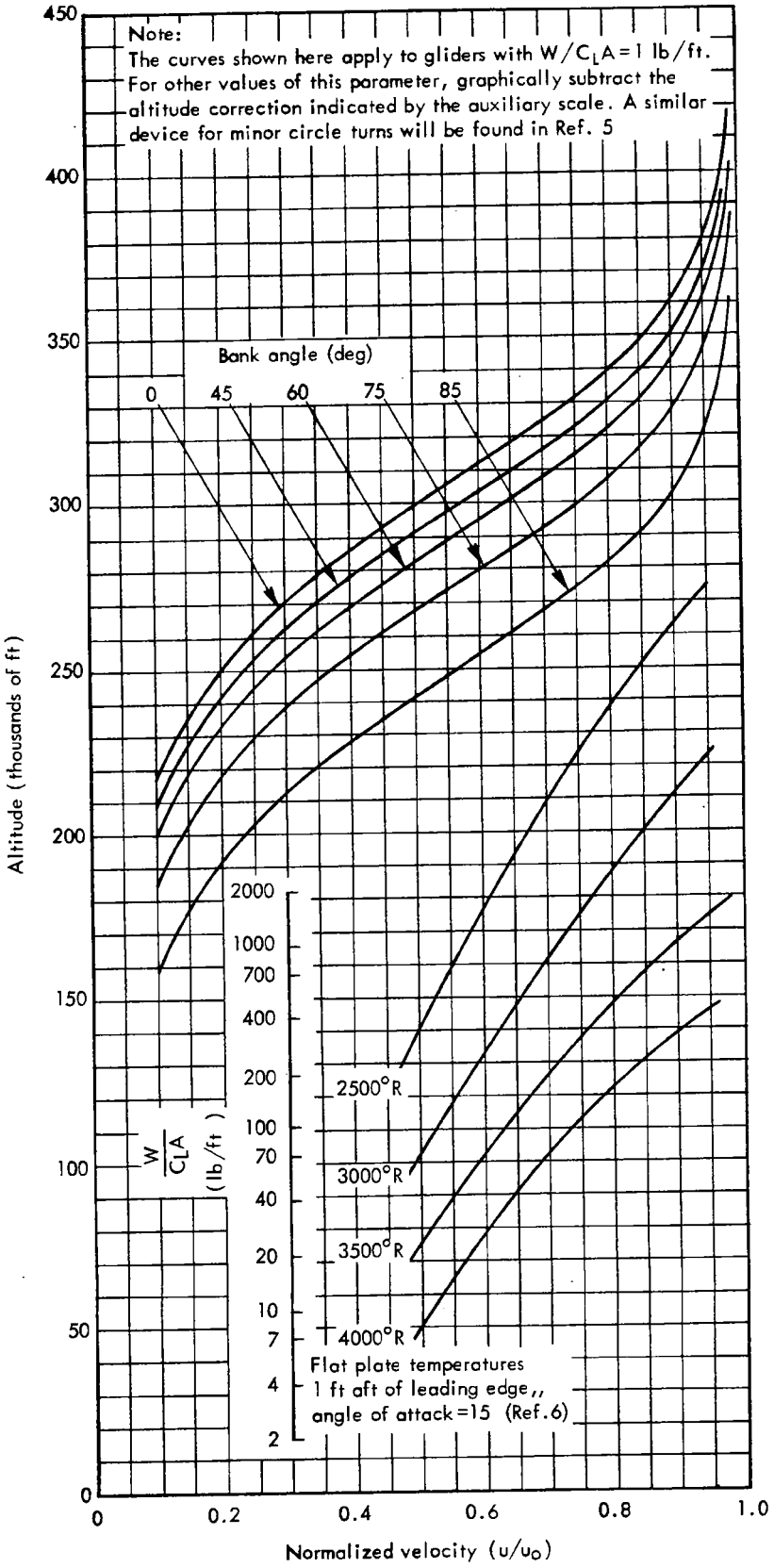

Fig. 3—Glide reentry trajectories for constant bank angle control

the point of maximum heating would still be the same as determined in Gazley's analysis.[7]

Vehicle time of flight can be found by writing an expression for the drag force,

$$D = \frac{1}{2} \rho_o e^{-\beta h} u^2 C_D A$$

and, substituting the expression for $e^{\beta h}$ from above, the differential equation relating velocity and time of flight is generated.

$$\frac{1}{g} \frac{du}{dt} = - \frac{1 - u^2/u_o^2}{\frac{L}{D} \cos \phi}$$

Integrating from an initial velocity and defining the time at the initial velocity as t = 0, the time of flight is given by

$$t = \frac{u_o (L/D) \cos \phi}{2 g} \log_e \frac{(1 - u/u_o)(1 + u_i/u_o)}{(1 + u/u_o)(1 - u_i/u_o)} \qquad (6)$$

Selected times of flight for various initial velocities are shown in Fig. 4. Note from this result that the time decreases to zero when the bank angle approaches 90 deg or L/D approaches zero. Under actual flight conditions, this trend would not hold. The equations yield such a result because the path angle would not be small when (L/D) cos ϕ approaches zero; this violates an assumption made earlier. Under these conditions, the trajectory would more closely resemble a ballistic entry into the atmosphere than a lifting trajectory. Thus, this analysis would probably be in error when vehicles with low L/D are very steeply banked; that is, when the component of lift along the

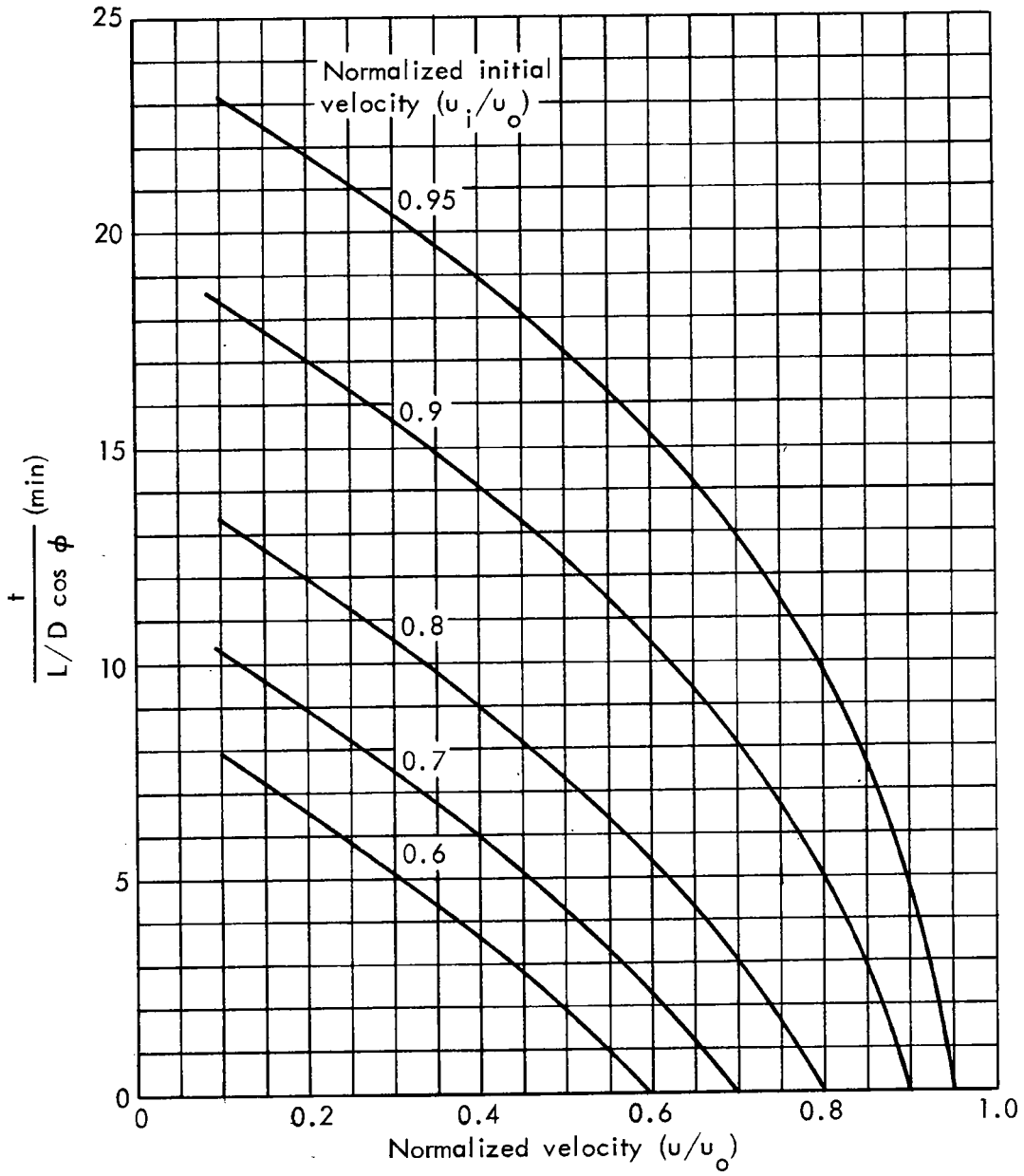

Fig.4—Time of flight

local vertical is small. A separate analysis will be performed in a later section of this paper to consider such flight regimes. In this section, the bank angle will be varied, but only up to a value slightly less than 90 deg for the range of lift-to-drag ratios of interest ($1 \leq L/D \leq 4$).

The solution for the path length is very similar to that for the time of flight, in that

$$\frac{du^2}{ds} = - \frac{2\, g\, (1 - u^2/u_o^2)}{(L/D)\, \cos \phi}$$

Integrating, and noting $u_o^2 = R_o g$,

$$s = \frac{1}{2} R_o\, (L/D)\, \cos \phi\, \log_e \frac{1 - u^2/u_o^2}{1 - u_i^2/u_o^2} \qquad (7)$$

The path length, s, is shown for various parameter values in Fig. 5. Note that for initial velocities of about $0.95\, u_o$, most of the distance to be flown has been covered by the time the vehicle slows down to $u \tilde{=} 0.6\, u_o$. Thus, it would appear that the effects of L/D for <u>covering distance</u> is greatest at high velocities, and thus a high L/D at low velocities does not contribute much in large scale maneuvers.

The downrange and siderange distances for constant bank angle control are found by noting that

$$\frac{dx}{du} = \frac{ds}{du} \cos \omega, \quad \frac{dy}{du} = \frac{ds}{du} \sin \omega,$$

where x is the distance traveled in the original direction of motion (downrange distance) and y is the distance traveled perpendicular to

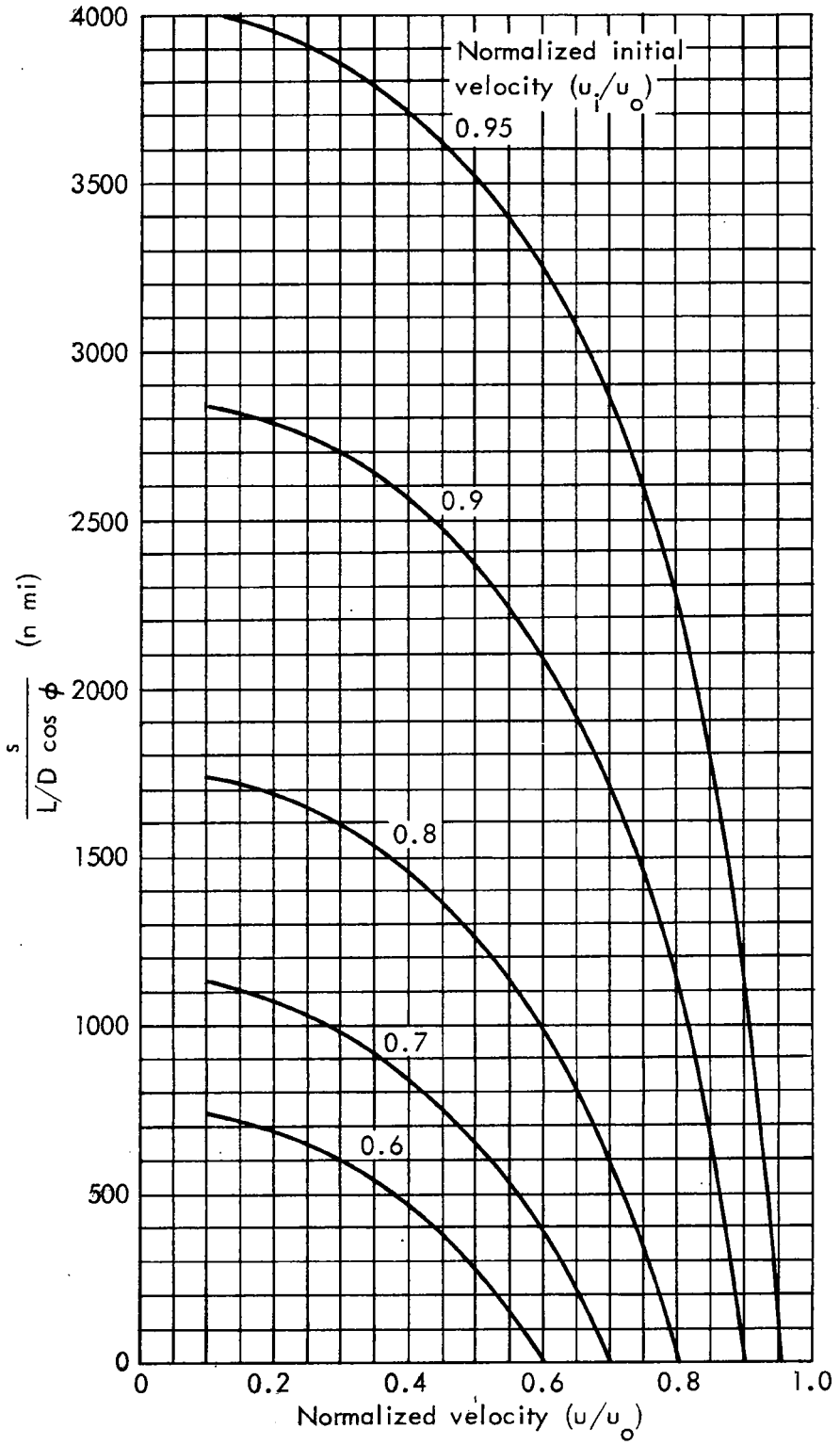

Fig. 5—Flight path length

the original direction of motion (siderange distance). Differentiating equation 7 with respect to velocity.

$$g \frac{ds}{du} = \frac{u \, (L/D) \cos \phi}{1 - u^2/u_o^2}$$

and substituting into the differential equations for crossrange and downrange distance (to eliminate the variable of vehicle heading angle), a pair of differential equations is generated relating velocity and distance.

$$g \frac{dx}{du} = \frac{u}{1 - u^2/u_o^2} \, (L/D) \cos \phi \cos \left(\frac{L}{D} \sin \phi \log_e u_i/u\right) \qquad (8)$$

$$g \frac{dy}{du} = \frac{u}{1 - u^2/u_o^2} \, (L/D) \cos \phi \sin \left(\frac{L}{D} \sin \phi \log_e u_i/u\right) \qquad (9)$$

These equations may be solved by making the substitutions

$$z = k \log (u/u_i), \; k = \frac{L}{D} \sin \phi$$

and expanding the result into an infinite series that is uniformly convergent in the region of interest. After integrating term by term and imposing limits,

$$g \frac{\tan \phi}{R_o} \, x = \sum_{n=1}^{\infty} (u/u_o)^{2n} \sin \left(\frac{L}{D} \sin \phi \log \frac{u}{u_i} + \tan^{-1} a \, n\right)$$

$$- \sum_{n=1}^{\infty} (u_i/u_o)^{2n} \frac{a \, n}{\sqrt{1 + a^2 \, n^2}} \qquad (10)$$

$$g \frac{\tan \phi}{R_o} \quad y = \sum_{n=1}^{\infty} (u/u_o)^{2n} \sin \left(\frac{L}{D} \sin \phi \log \frac{u}{u_i} - \tan^{-1} \frac{1}{an} \right)$$

$$+ \sum_{n=1}^{\infty} (u_i/u_o)^{2n} \frac{1}{\sqrt{1 + a^2 n^2}} \qquad (11)$$

where $a = \frac{2}{(L/D) \sin \phi}$

These functions are shown in Figs. 6, 7, 8, and 9 for L/Ds ranging from 1 to 4. Velocity is shown as a parameter, with the initial velocity assumed to be $0.98\ u_o$. The maximum cross range is achieved with a bank angle of 45 deg, as observed by Slye,[2] but only at low lift-to-drag ratios. At high L/Ds with a low terminal velocity, the maximum side range appears to be attained when the bank angle is somewhat less than 45 deg. Also at high lift-to-drag ratios, the vehicle proceeds along its spiraling path far enough to achieve large heading changes, even completely reversing its direction of flight by the time it reaches very low velocities ($0.2 \lesssim u/u_o \lesssim 0.3$).

It was assumed earlier that the vehicle would not depart too far from its original entry plane. But our results indicate that this would not be a good assumption for trajectories that are allowed to proceed to low terminal velocities where the vehicle has a high L/D and employs a medium bank angle of ~45 deg. Thus, those results shown that involve crossrange distances of more than 2000 n mi or so are probably approximate at best. However, if the primary application of these results is for studying synergetic plane changing, such a restriction would not place serious limits on the usefulness of this

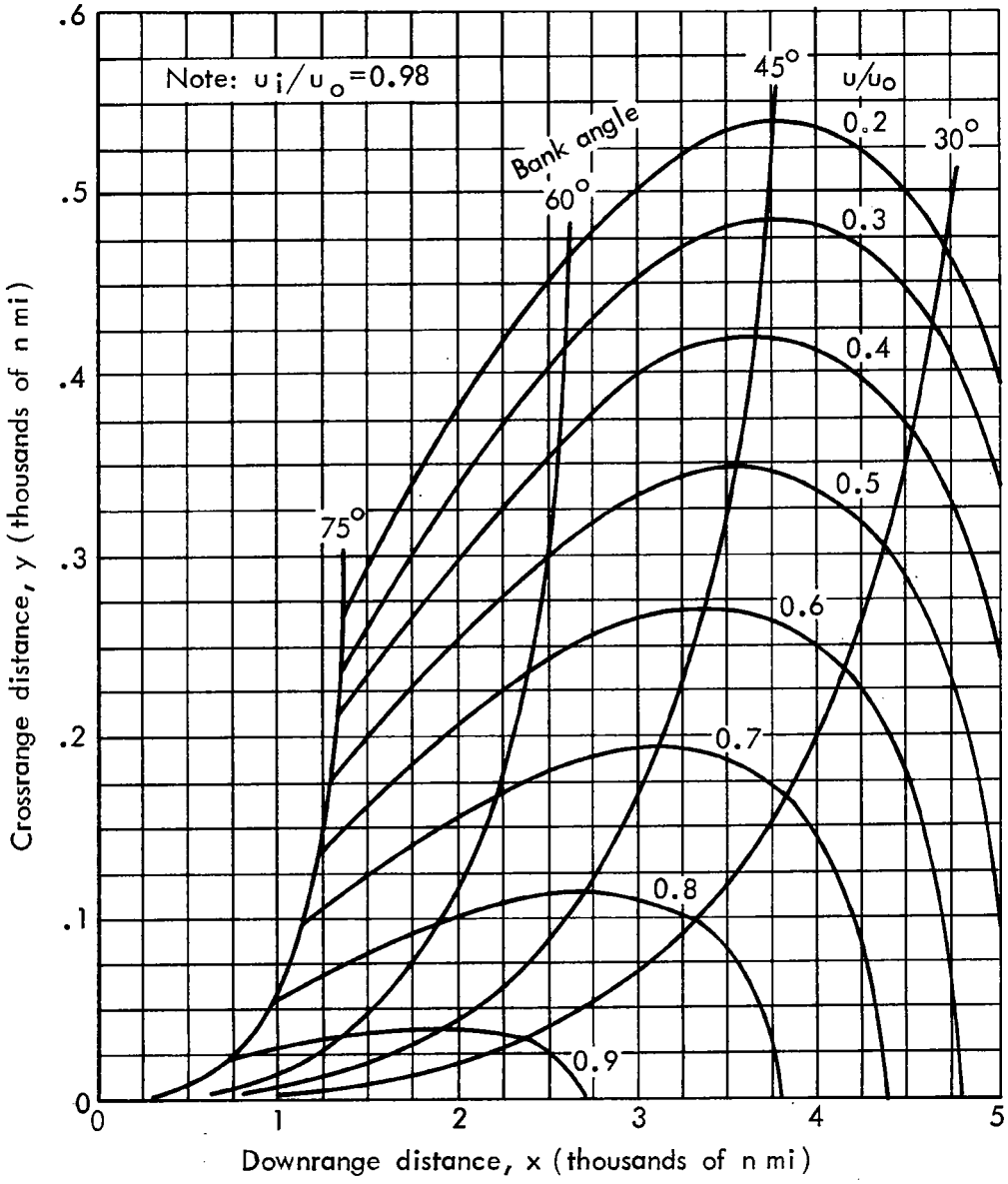

Fig.6—Ground trace during turn, L/D = 1

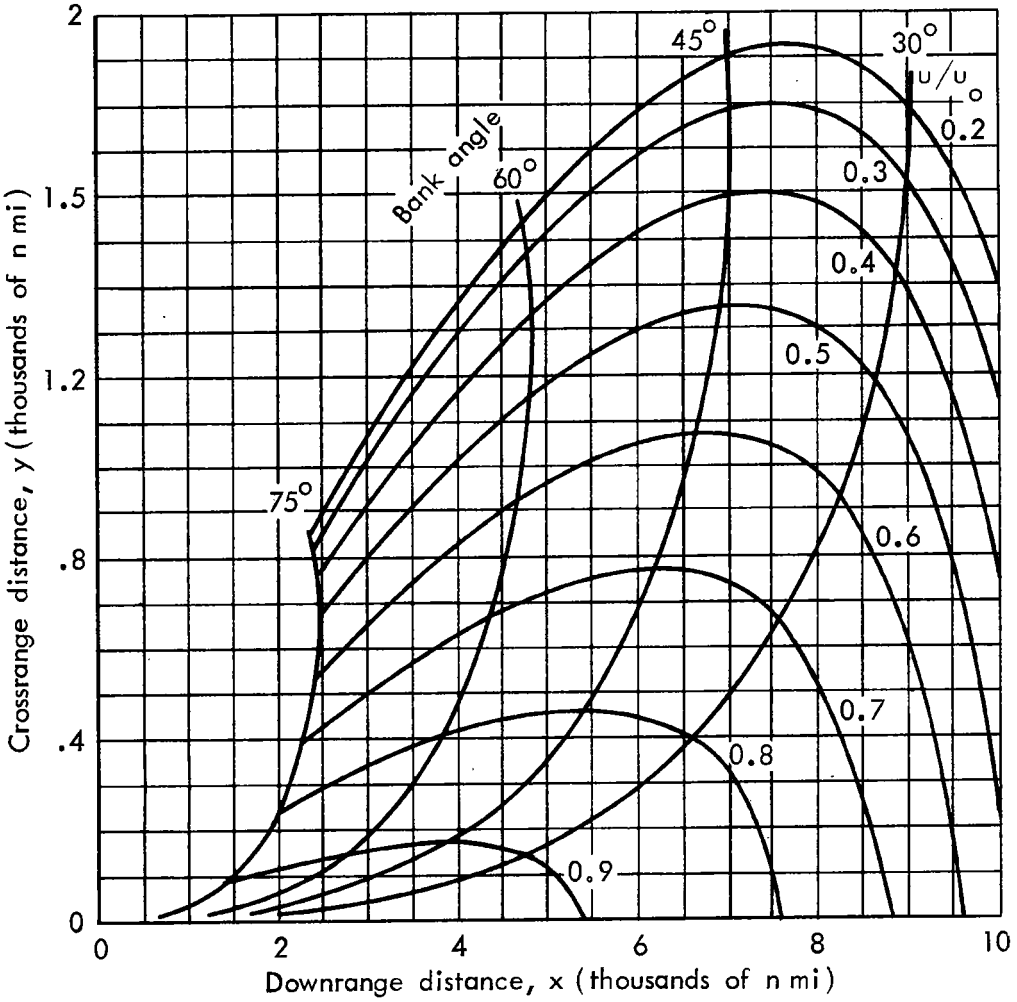

Fig.7—Ground trace during turn, L/D = 2

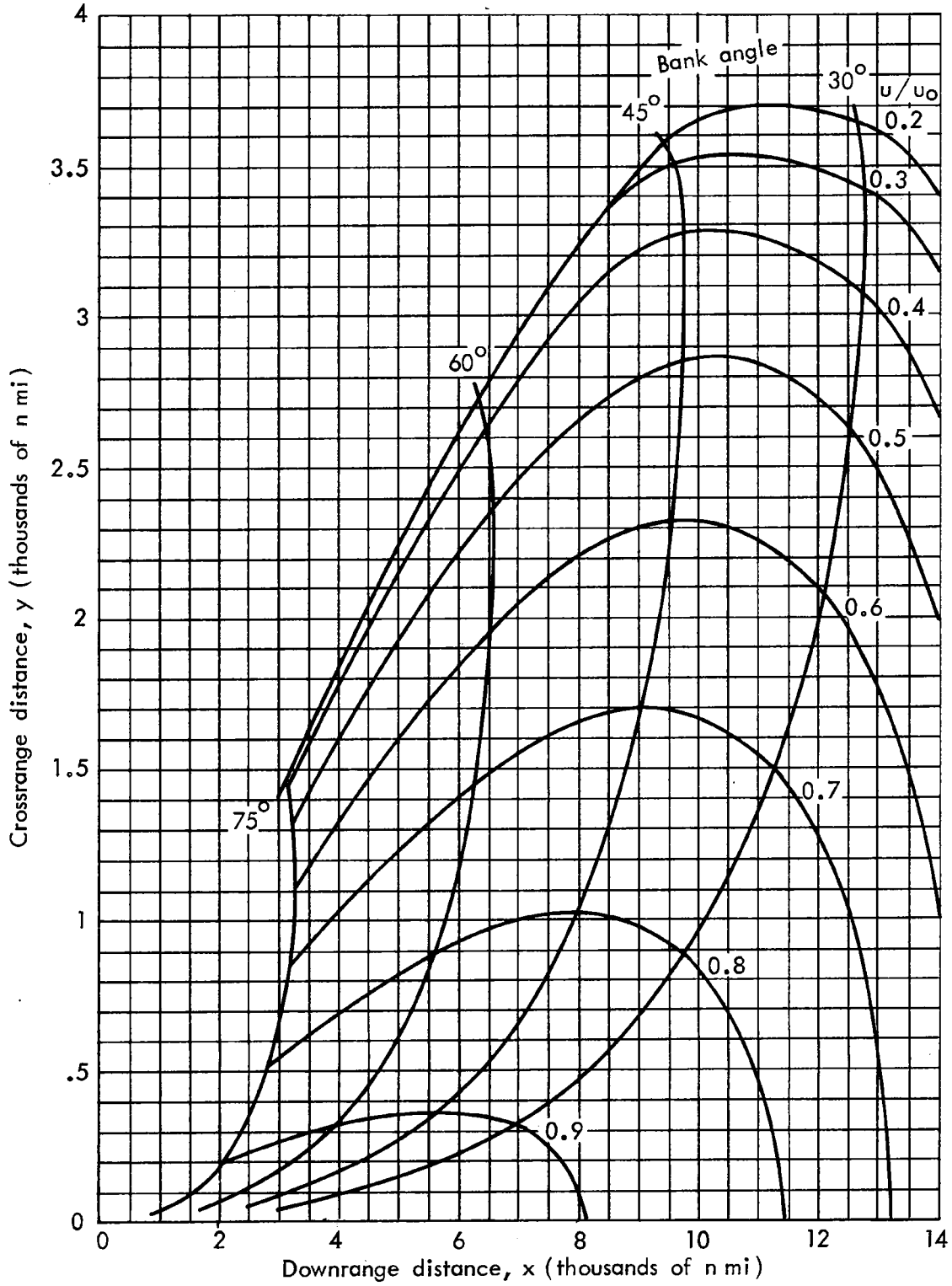

Fig.8—Ground trace during turn, L/D = 3

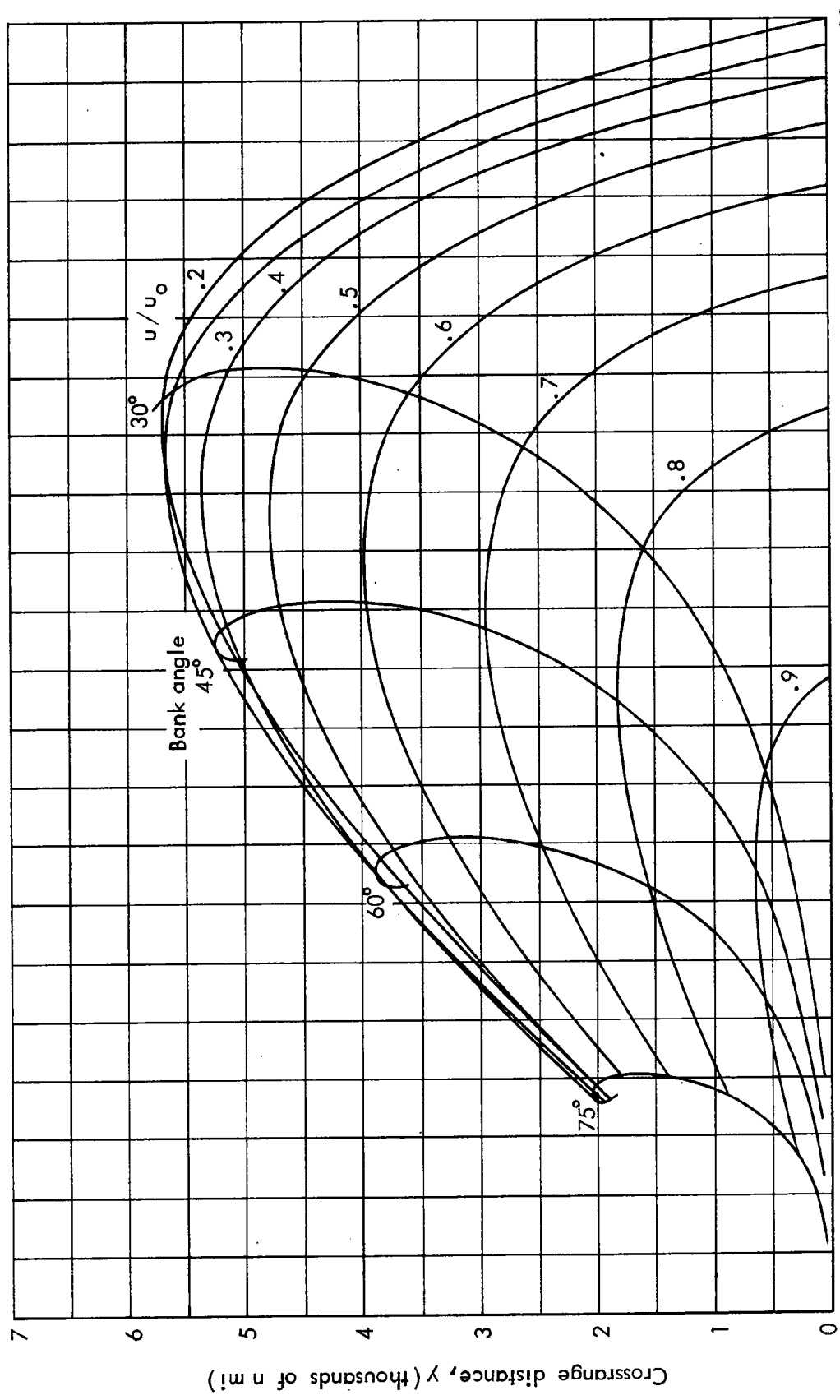

Fig. 9—Ground trace during turn, L/D = 4

investigation, because in this case the heading change desired may occur well before the vehicle departs very far from the original orbital and entry plane.

IV. TRAJECTORIES FOR BANK ANGLES OF 90 DEGREES

In this section we will discuss the special case of constant bank angle turns where ϕ = 90 deg. In this part of the analysis, the path angle may not be small, and the equations developed above may not allow the analyst to estimate trajectory characteristics with reasonable accuracy. Here, we will make other assumptions that permit closed form solutions to the equations of motion. These solutions should be useful in making estimates of vehicle performance when the bank angle is 90 deg. As previously noted, the assumption that the path angle is very small during reentry stems from the fact that there is some lift along the local vertical, and this lift force tends to keep the path angle small for a large portion of the flight through the atmosphere. In this discussion, we will assume that the path angle may be nonzero, but that it is constant ($d\gamma/dt = 0$). These assumptions are similar to those made in analyzing the ballistic reentry situation.[7] Additionally, we will assume that the acceleration due to gravity along the flight path is small compared to the deceleration due to drag, that the acceleration due to gravity is constant in the region of interest, and that the control variables are constant throughout the flight (specifically, the bank angle is 90 deg).

Under these conditions the equations of motion become

$$\frac{1}{2g}\frac{du^2}{ds} = \frac{1}{g}\frac{du}{dt} = -\frac{D}{W} = -\frac{1}{2}\rho_o e^{-\beta h} u^2 C_D A/W \qquad (12)$$

$$\frac{u}{g}\frac{d\omega}{dt} = \frac{L}{W} = \frac{1}{2}\rho_o e^{-\beta h} u^2 C_L A/W \qquad (13)$$

In finding the altitude-velocity profile, the density factor, σ, is used to describe the distribution of atmospheric density, in that $\sigma = e^{-\beta h}$. From the geometry

$$\frac{dh}{dt} = u \sin \gamma, \quad \frac{d\sigma}{dt} = -\beta \sigma \frac{dh}{dt}$$

and rearranging to eliminate time as a variable,

$$\frac{du}{d\sigma} = \frac{1}{2} \frac{g \rho_o C_D A}{W \sin \gamma} u$$

where γ is the flight path angle defined positive in an upward direction. Integrating from a very high altitude where the atmospheric density is essentially zero, and the velocity is the reentry velocity, u_r,

$$\frac{u}{u_r} = \exp \left(\frac{g \rho_o}{\beta \frac{2W}{C_D A} \sin \gamma} e^{-\beta h} \right) \tag{14}$$

This result is shown in Fig. 10 for $(W/C_D A) \sin \gamma = 1$. An auxiliary scale indicates the altitude decrement that should be used for other values of the ballistic coefficient and path angle. In the previous section, where there was lift along the local vertical, the altitude-velocity profile exhibited a singularity at orbit velocity. In the case of a nonzero reentry angle, the singularity exists at the reentry velocity because the altitude at this velocity was assumed to be essentially infinite. To avoid difficulties in using the information in a practical problem, we shall later use the term initial

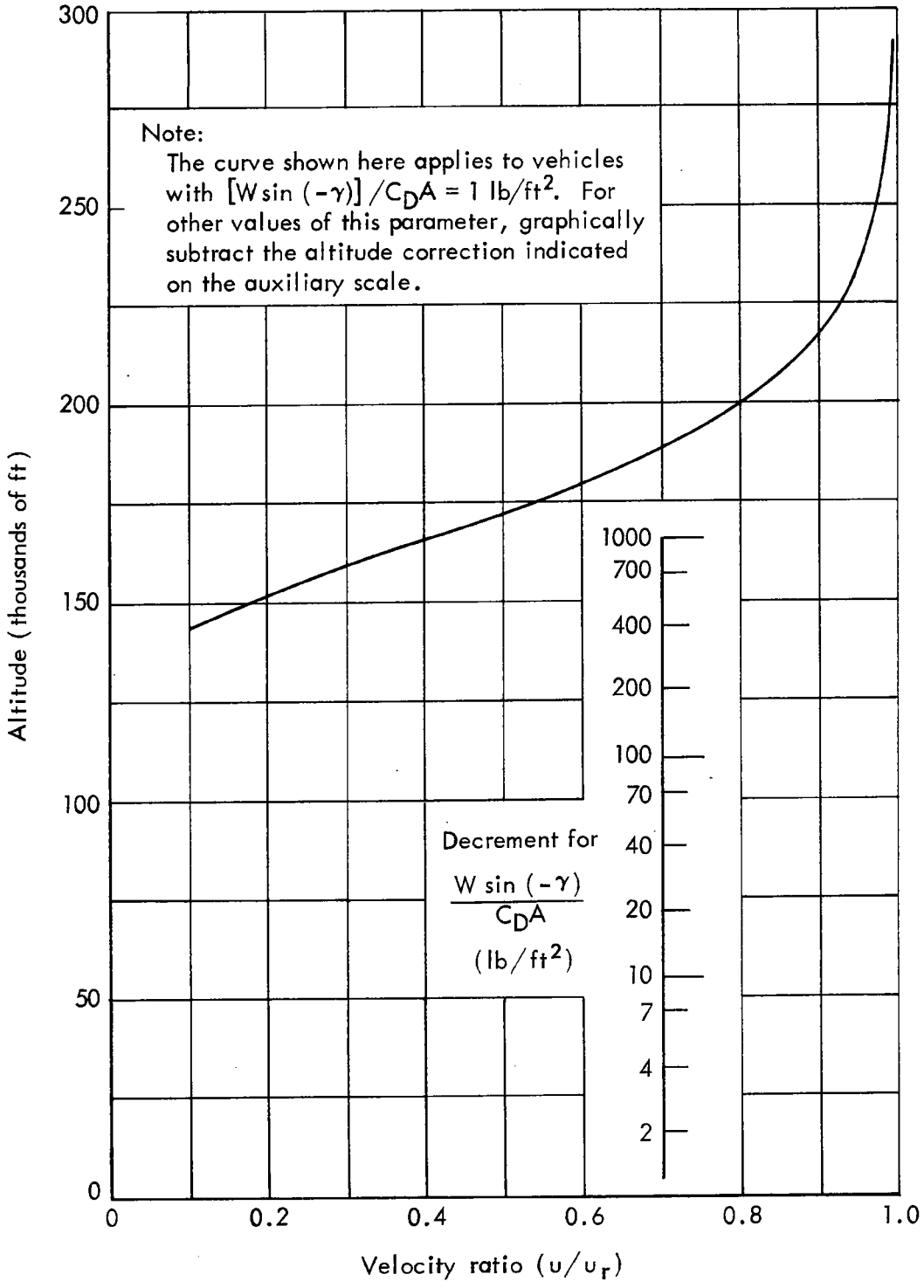

Fig. 10—Altitude velocity profiles for $\phi = 90°$ or purely ballistic reentries

velocity as that velocity where the dynamic interaction of the vehicle and atmosphere begins to be of interest, and where most of the assumptions made in this investigation become reasonably valid.

The vehicle heading is found by combining Equations 12 and 13 to eliminate time as a variable, and then integrating,

$$\omega = (L/D)\ \log_e u_r/u \tag{15}$$

This result is nearly the same as that obtained at lower bank angles (Eq. 4) except that in this instance, the full force of lift is a applied sideways. Fig. 2 (p. 8) can be used to show the heading angle for various velocities and lift-to-drag ratios by setting $\sin \phi = 1$. If a large change in heading is desired with only a small velocity loss due to drag, then a high L/D value would be beneficial.

The path length is found by noting that

$$e^{-\beta h} = \frac{\log_e u/u_r}{\left(\frac{1}{2}\frac{\rho_o C_D A}{\beta W \sin \gamma}\right)}$$

and can be substituted in equation 12 to obtain

$$\frac{du}{ds}^2 = -\beta \sin \gamma\, u^2 \log_e (u/u_r)^2$$

Integrating,

$$s = \left.\frac{\log_e \log_e (u_r/u)^2}{\beta \sin (-\gamma)}\right]_{u_i}^{u} = \frac{1}{\beta \sin (-\gamma)} \log_e \left[\frac{\log_e u_r/u}{\log_e u_r/u_i}\right] \tag{16}$$

Again, a singularity exists at the reentry velocity, and to use the results one must consider use of an initial velocity slightly less than reentry velocity to avoid an undefined path length.

The time of flight when the bank angle is 90 deg may be found by recalling that

$$\frac{d\sigma}{dt} = (-\beta \sin\gamma)\, u\, \sigma, \quad \sigma = e^{-\beta h}$$

Substituting into this expression the solution for the velocity-altitude profile derived earlier,

$$u/u_r = \exp\left[-\frac{g\rho_o C_D A}{2\beta W \sin(-\gamma)} e^{-\beta h}\right] = e^{-b\sigma}$$

Then the differential equation to be solved becomes

$$\frac{d\sigma}{dt} = (-\beta u_r \sin\gamma)\, e^{-b\sigma}$$

and integrating, the solution is in the form of an exponential integral.

$$(-\beta\, u_r \sin\gamma)\, t = \int_{b\sigma_i}^{b\sigma_f} \frac{e^z}{z}\, dz$$

The limits in this form are somewhat awkward, but may be revised in terms of initial, reentry, and final velocities by noting that $\log_e u_r/u = b\sigma$. Thus,

$$(-\beta u_r \sin\gamma)t = \int_{\log \frac{u_r}{u_i}}^{\infty} \frac{e^z}{z}\, dz - \int_{\log \frac{u_r}{u_f}}^{\infty} \frac{e^z}{z}\, dz \qquad (17)$$

is the final result and use of tables[8] will yield numerical values for the time of flight. Several examples are to be found in Fig. 11.

The load factor (L/W) on the glider during its turn with a 90 deg bank angle is found by noting that

$$L/W = 1/2\ \rho_o\ u^2\ \frac{C_L A}{W}\ \sigma$$

and substituting for the dummy variable, σ,

$$L/W = R_o \beta\ (L/D)\ \sin\ (-\gamma)\ (u^2/u_o^2)\ \log_e\ (u_r/u) \qquad (18)$$

when the reentry velocity is about on the order of orbit velocity. The ratio of load factor to the sine of the reentry angle is shown in Fig. 12 as a function of the velocity. It can be shown that the maximum value of the load factor always occurs at a velocity corresponding to $u/u_r = e^{-1/2} = 0.603$, just as in a purely ballistic reentry. The trends to be observed are that the normal load factor increases with L/D and reentry angle. Thus, to limit load factors to reasonable values for reentries with ϕ = 90 deg, a very small reentry angle would be desirable. Note that in the previous analysis where bank angles were less than 90 deg, the load factors were considerably smaller than those shown here. Thus, the normal load factor is also quite sensitive to the bank angle, when it is in the neighborhood of 90 deg.

The crossrange and downrange distances of travel are found by a method similar to that used earlier when the bank angle was allowed to be less than 90 deg. First, note that

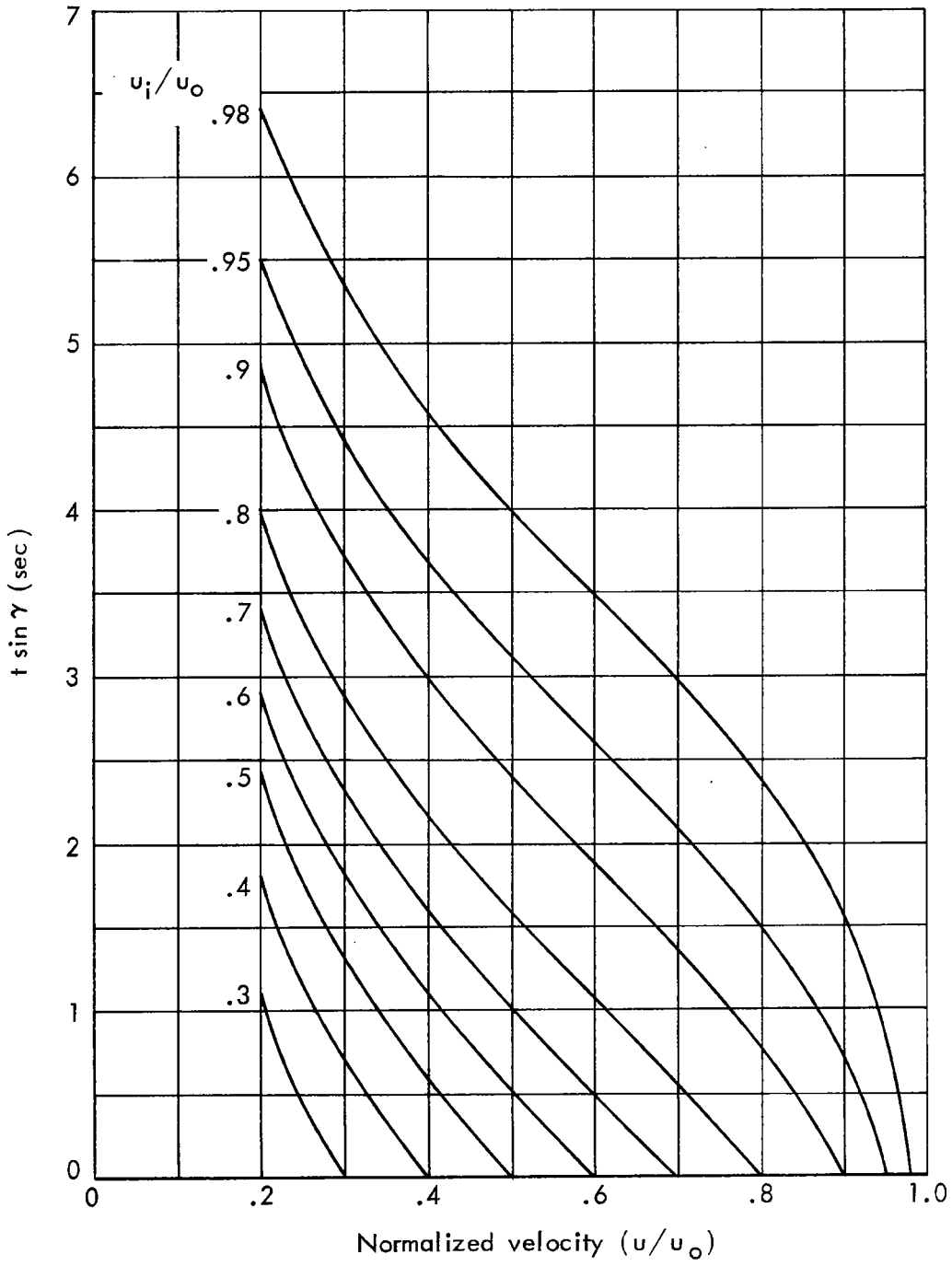

Fig. 11—Time of flight ($\phi = 90°$)

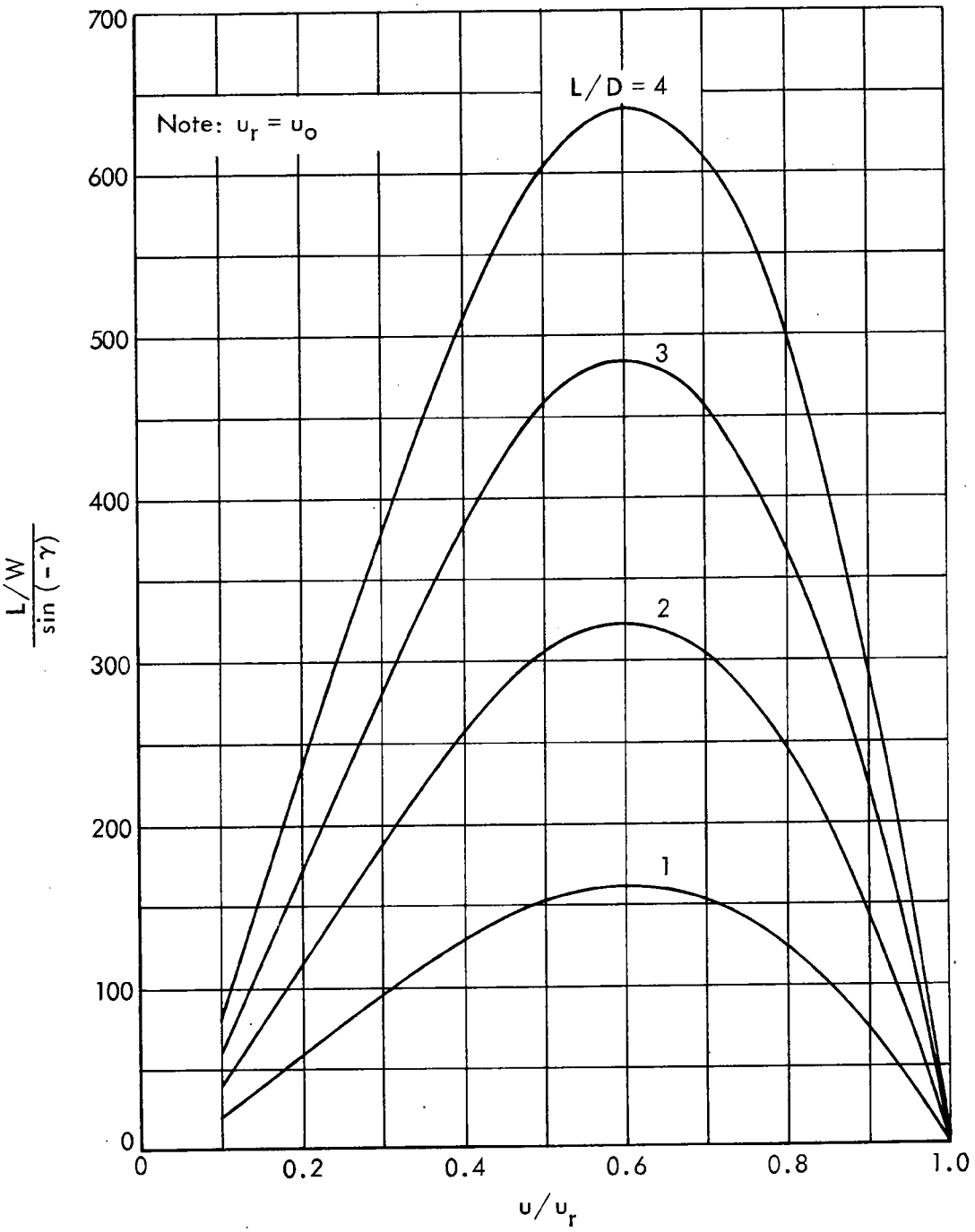

Fig. 12—Normal load factor for $\phi = 90°$

$$\frac{dy}{du} = \frac{ds}{du} \sin \omega, \quad \frac{dx}{du} = \frac{ds}{du} \cos \omega$$

and that by differentiating the path length with respect to velocity,

$$\frac{ds}{du} = \frac{1}{u \beta \sin \gamma \log_e (u_r/u)}$$

and substituting, the differential equations to be solved are

$$\frac{dy}{du} = \frac{\sin \left[\log_e (u_r/u)^{L/D} \right]}{u \beta \sin \gamma \log_e (u_r/u)}$$

$$\frac{dx}{du} = \frac{\cos \left[\log_e (u_r/u)^{L/D} \right]}{u \beta \sin \gamma \log_e (u_r/u)}$$

Using the substitution,

$$z = \log_e (u/u_r)^{L/D}$$

these equations reduce to the familiar sine and cosine integrals that are well tabulated.[8]

$$y = \frac{1}{(L/D) \beta \sin \gamma} \left[Si(\frac{L}{D} \log_e \frac{u_r}{u_f}) - Si(\frac{L}{D} \log_e \frac{u_r}{u_i}) \right] \qquad (19)$$

$$x = \frac{1}{(L/D) \beta \sin \gamma} \left[Ci(\frac{L}{D} \log_e \frac{u_r}{u_f}) - Ci(\frac{L}{D} \log_e \frac{u_r}{u_i}) \right] \qquad (20)$$

where u_f is the final velocity of interest, u_r is the vehicle velocity well above the atmosphere (reentry velocity), and u_i is that initial velocity (somewhat less than reentry velocity) where the interaction of the vehicle and the atmosphere begins to be

appreciable and the assumptions of this analysis apply. Thus, $u_i < u_r$.

Figures 13, 14, and 15 show the ground traces during steeply banked turns with final velocity as a parameter. The initial velocities are $u_i = 0.98\ u_r$, $0.95\ u_r$, and $0.9\ u_r$ respectively. Note that the greatest heading change that can be accomplished with the least amount of velocity loss requires the highest lift-to-drag ratio (L/D = 4 in this case). The side range achieved for a given final velocity is almost independent of L/D for final velocities greater than about $0.7\ u_r$. Thus, the higher L/Ds, if available, are used only to turn the vehicle faster when the bank angle is 90 deg. If large side ranges are desired, a more moderate bank angle would be used, and the results of the previous section would be applicable.

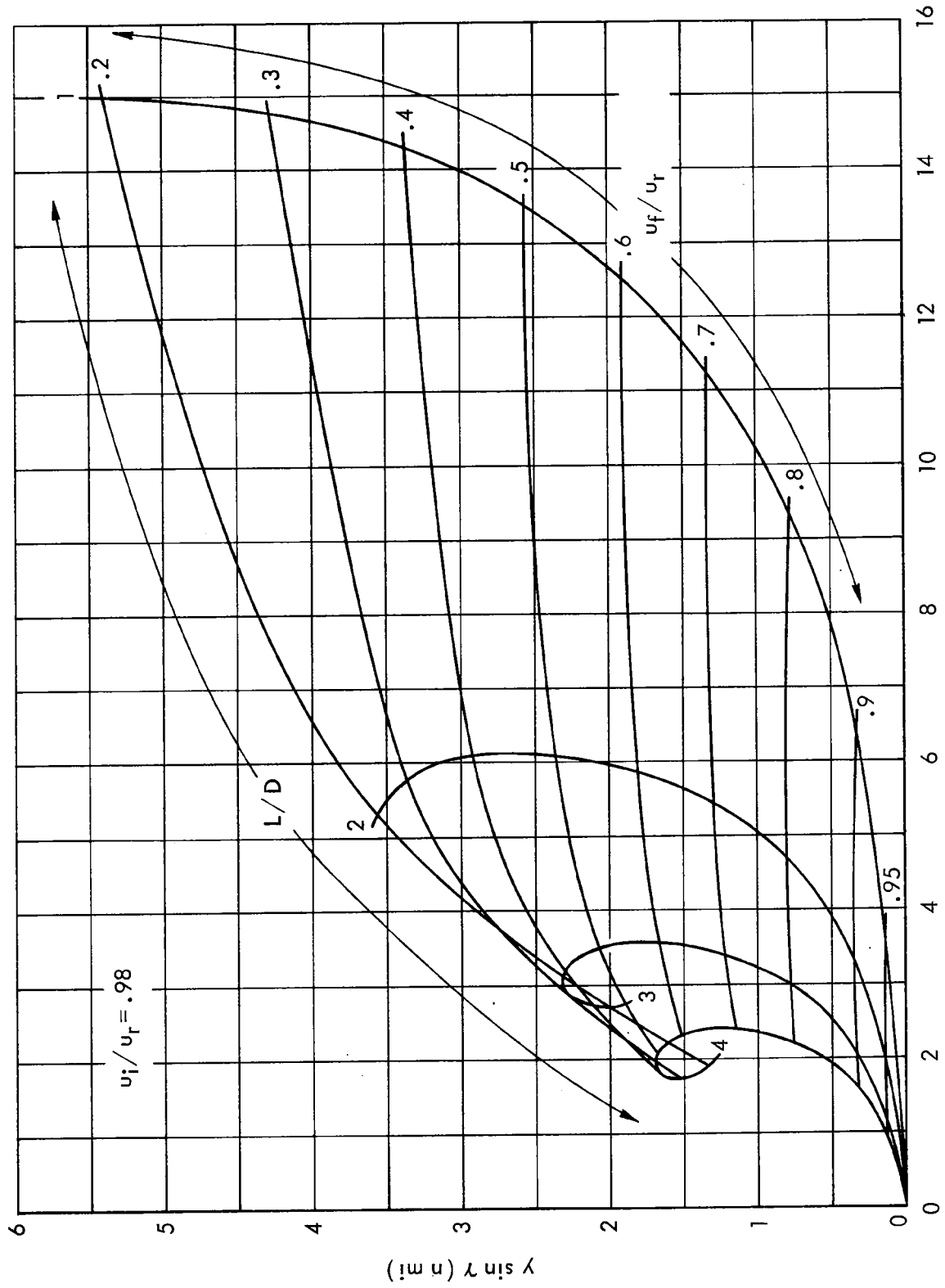

Fig. 13—Ground trace for $\phi = 90°$ ($u_i = 0.98\, u_r$)

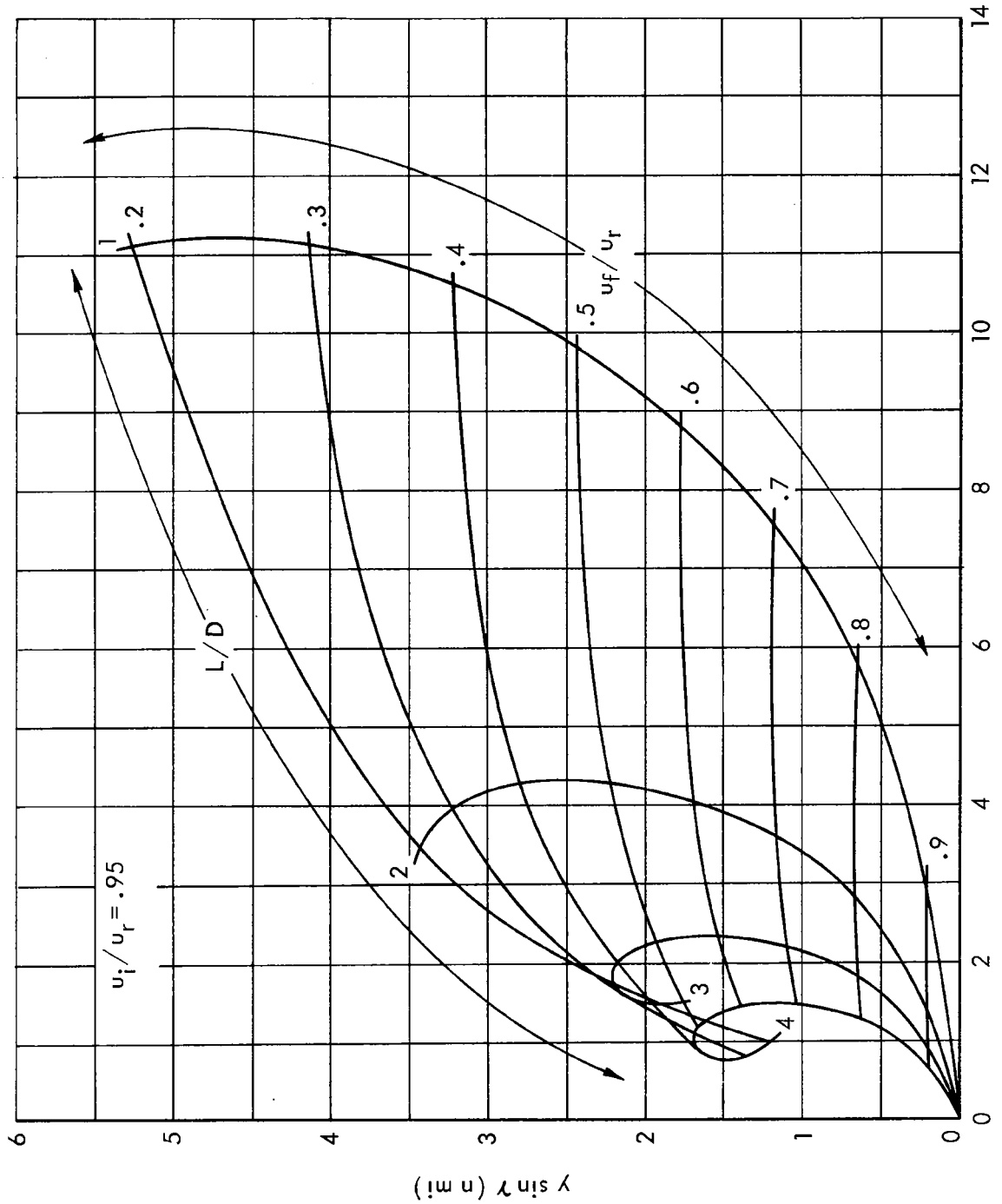

Fig. 14—Ground trace for $\phi = 90°$ ($u_i = 0.95\ u_r$)

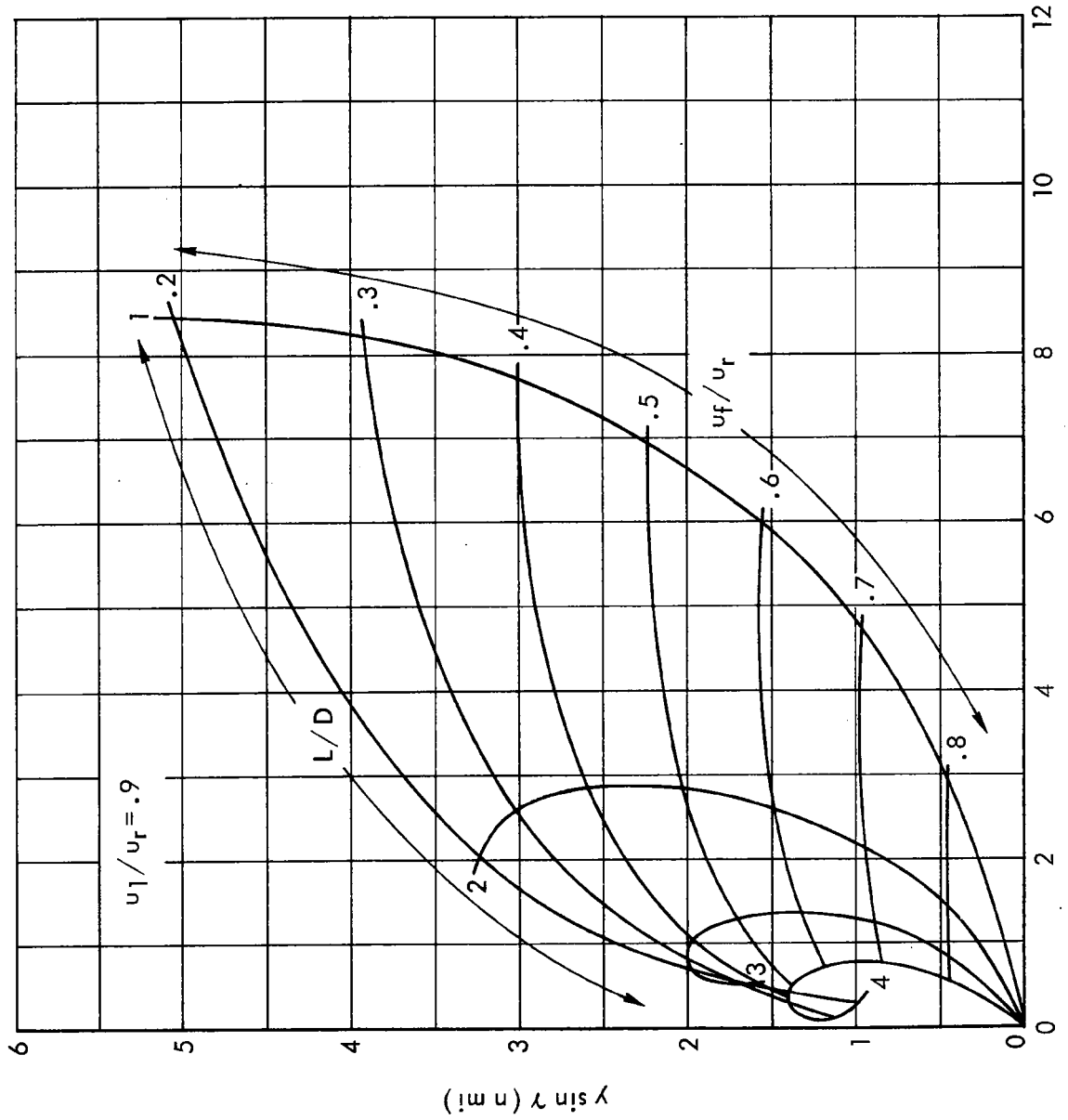

Fig. 15— Ground trace for $\phi = 90°$ ($u_i = 0.90\, u_r$)

V. HEATING TRENDS

To gain an insight into heating trends, we will assume that a given percentage of the total mechanical energy lost during the turn due to drag is converted into heat which is then transmitted to the vehicle. Gazley[7] has assumed that the fraction of total energy transferred as heat into the vehicle can be represented as a function of altitude. We will also make this assumption, but will not specify the exact function, since many analysts may have different functions that they consider appropriate, and, in practice, a detailed study would require prior specification of vehicle geometry, position on the vehicle, thermal protection system, etc. Using a general form of the transfer fraction (f), one may write the instantaneous heating rate indicator as

$$\frac{dQ}{dt} = f\, C_D\, \rho\, u^3 = \rho_o\, f\, C_D\, u^3\, e^{-\beta h} \tag{21}$$

To find the indicated heating rate in a simpler form, we merely substitute for $e^{-\beta h}$ in equation 21. For turns where $\phi < 90$ deg,

$$\frac{dQ}{dt} = \frac{2\, f\, (W/A)\, u\, (1 - u^2/u_o^2)}{\frac{L}{D}\, \cos \phi} \tag{22}$$

and for turns where $\phi = 90$ deg,

$$\frac{dQ}{dt} = 2\, f\, (W/A)\, (\sin \gamma)\, u^3 \log_e (u/u_r) \tag{23}$$

In both cases, the heating rate at a given velocity is directly proportional to wing loading. When the bank angle is less than 90 deg,

the heat rate is larger when the vertical component of lift to drag is small. This condition could arise from either a steep bank angle or a low vehicle lift-to-drag ratio, or both. When the bank angle is 90 deg, the heat rate is larger when the reentry path angle is steeper, and appears to be a much stronger function of velocity than in cases with moderate bank angles. An indication of total heat could be obtained by integrating these equations, but is not included in this study.

VI. FINAL COMMENTS

In this study we have presented a method of calculating turning trajectories for reentry vehicles. Because the method leads to closed form solutions, made possible by certain assumptions, the analysis has its limitations. However, the difference between a sophisticated computation and the results presented here will be very small, so long as the vehicle does not depart too radically from the initial reentry plane. Even at the larger side ranges, the model developed in this paper may be used to provide first-order estimates of vehicle performance.

There are other assumptions that would also permit closed form solutions. The assumptions that we have used have been made by many other analysts, however, and the errors from such sources are generally quite small. We assumed, for instance, that the acceleration due to gravity was constant at its sea level value in the region of interest, and also that the atmospheric density decayed exponentially with altitude. For both sections of this analysis, assumptions were made about the flight path angle, and the analysis would only be nearly correct when such assumptions apply. Fortunately, if synergetic plane changing is of interest, all of the assumptions made in this study appear to be reasonably good ones. A measure of how reasonable these assumptions are can be determined by comparing our results with various trajectory calculations performed by numerical methods not restricted by linearizing assumptions.[4]

The first comparison is between two methods for determining heading change as a function of vehicle velocity. Fig. 16 shows the

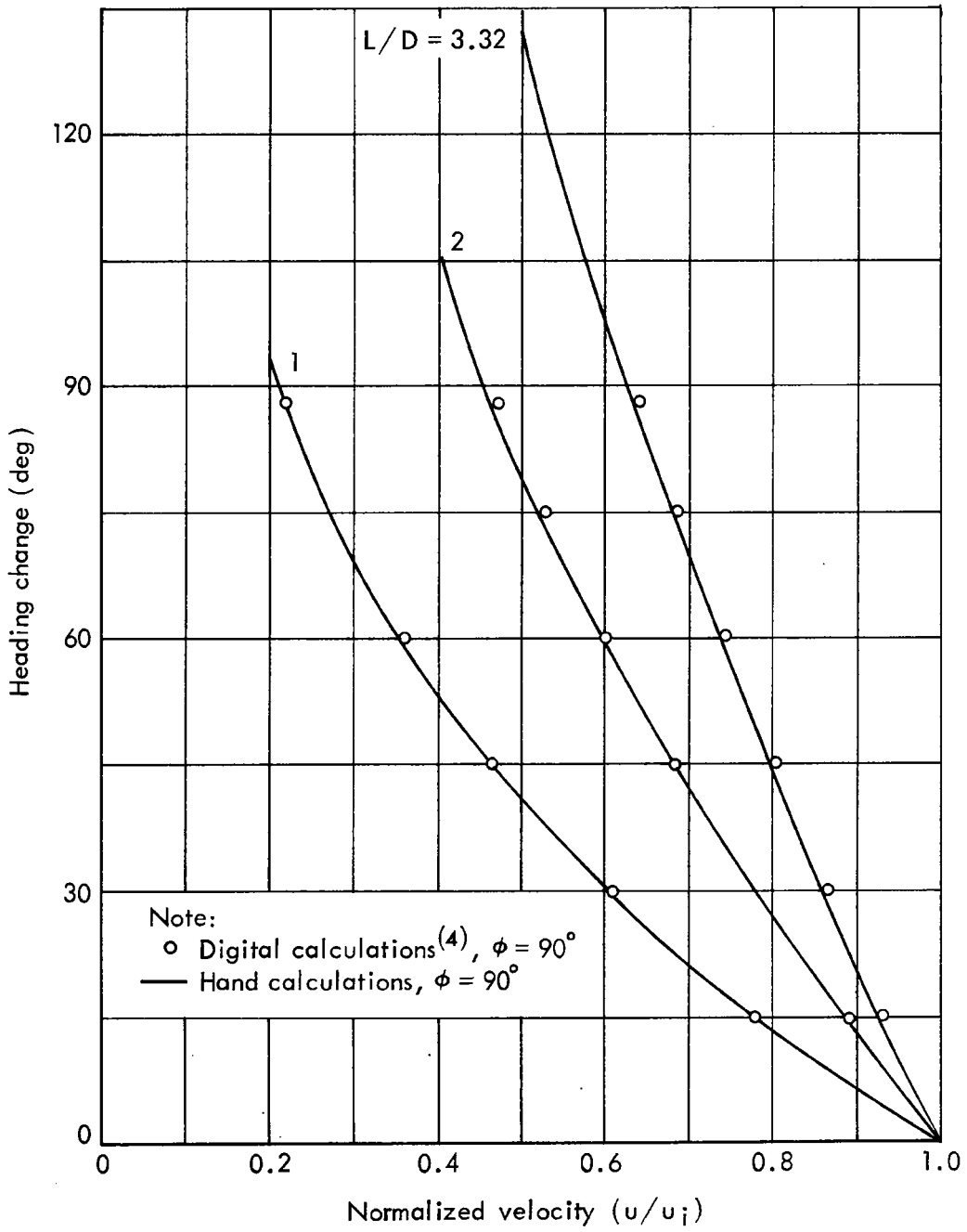

Fig. 16—Comparison of heading change calculations by two methods

results of this analysis for a 90 deg bank angle trajectory (solid lines) and calculations performed on a digital computer. The agreement between the two methods is good, and thus indicates that one may use hand calculations with confidence for determining heading changes for trajectories if the bank angle is 90 deg and the lift-to-drag ratio ranges from 1.0 to 3.32.

The altitude-velocity profiles calculated by our model and by a digital computer are compared in Fig. 17. The conditions for the comparison are noted on the figure. Although there is general agreement, the hand model predicts a higher altitude as the vehicle velocity decreases below about 0.8 u_r. The reason for this discrepancy, even though it is always less than 15,000 ft in this case, is that the hand analysis is based on the assumption that the path angle remains constant. According to digital calculations, the path angle is becoming larger (in a downward direction). Thus, it appears that at the lower velocities, the hand model might not be accurate enough for some users. Fortunately in this example, however, there would not be much interest in velocities lower than those shown, because the vehicle heading has undergone a 90 deg change by the time its velocity has decreased to about half its reentry velocity. For higher lift-to-drag ratios, even less velocity would be lost before such large heading changes would be achieved, and the agreement would probably be good throughout the region of interest.

For comparison of velocity-altitude profiles when the bank angle is less than 90 deg, we have chosen Shaver's "bounded" results[4] (Fig. 17). Hand calculations are compared with two trajectories where, on the average, the bank angle is about 85 deg (Fig. 18). The agreement

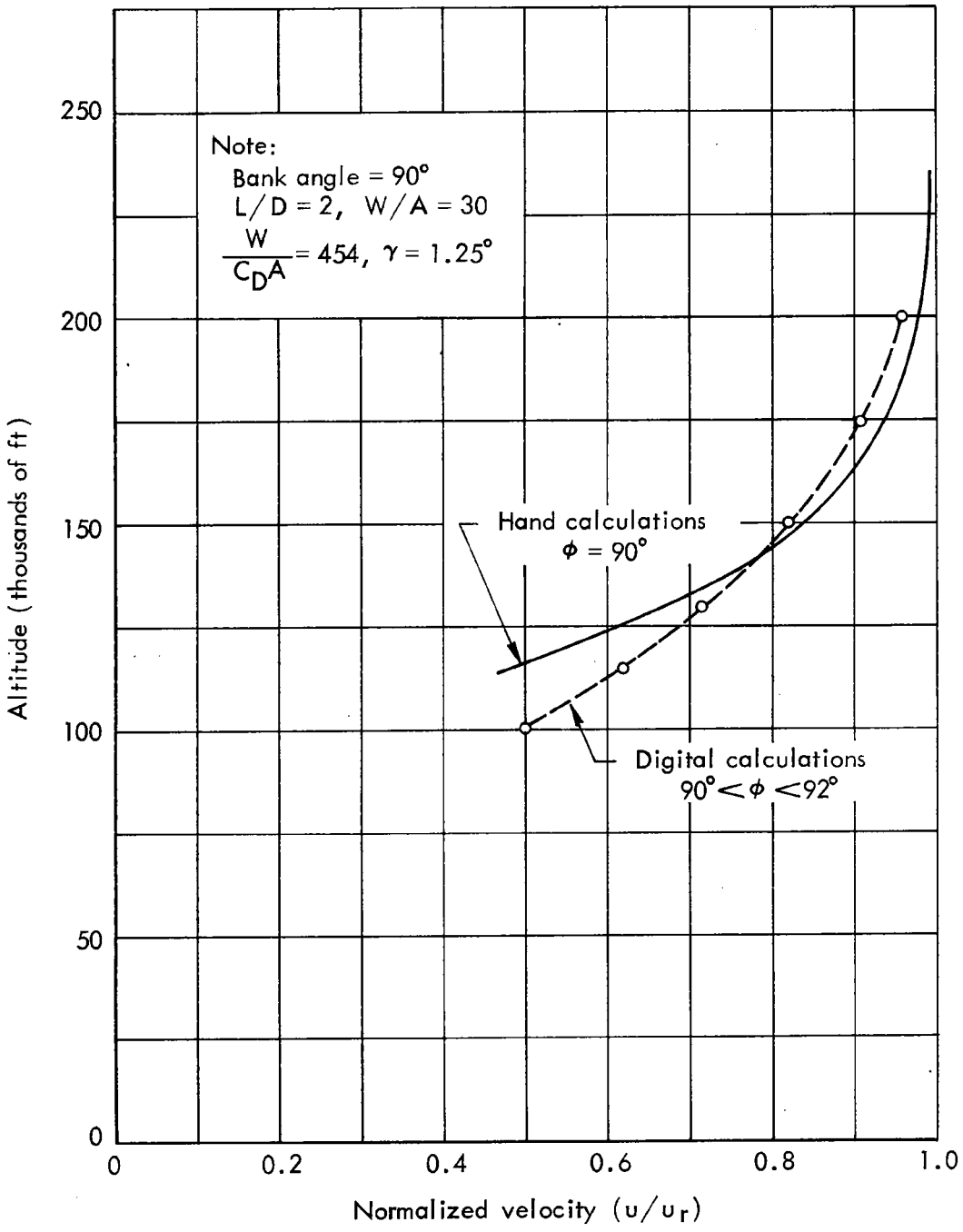

Fig. 17—Comparison of velocity - altitude profiles, $\phi = 90°$

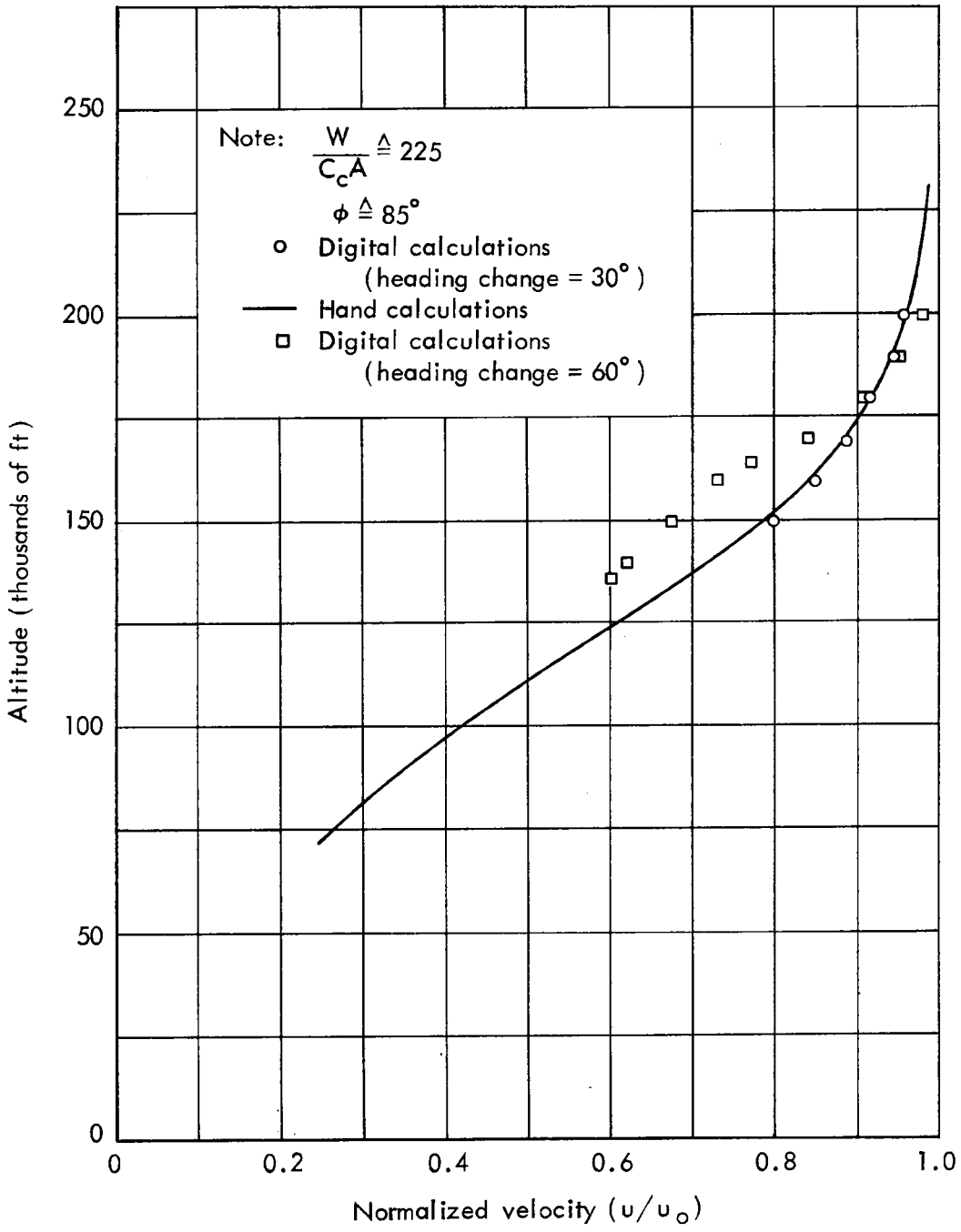

Fig. 18 — Comparison of altitude-velocity profiles, $\phi = 85°$

is excellent for the trajectory where the heading change is about 30 deg. For the case with a 60 deg heading change, agreement is not as good because the bank angle varied in the digital calculations. At the higher velocities (about 0.9 u_o), the bank angle varied from 83 to 85 deg, and the digital calculations show the vehicle beginning to level off more than the hand model would indicate. At the lower velocities, when the bank angle was allowed to approach 90 deg, the digital calculations tend to more closely approximate the hand model predictions. The altitude-velocity profile is very sensitive to bank angle variations, as we observed earlier, and one should expect variations to be large if the bank angle is modulated in flight. The largest variation appears to be about 20,000 ft above the hand predictions. The digital results also indicate a slight tendency of the vehicle to "skip," an effect that would not be evident in a first-order hand calculation. Only second-order analyses such as those performed by Loh on an in-plane descent would give indications of skipping.[9]

In general, there appears to be reasonable agreement, good enough for advanced planning purposes, between digital and hand calculations, so that the analyst may make use of simple calculations to estimate trajectory parameters for glide reentry problems.

REFERENCES

1. Loh, W. H. T., "Dynamics and Thermodynamics of Reentry," Journal of the Aerospace Sciences, October 1960, pp. 748-762.

2. Slye, R. E., An Analytical Method for Studying the Lateral Motion of Atmosphere Entry Vehicles, National Aeronautics and Space Administration, TN D-325, September 1960.

3. Mandell, Donald S., "Maneuvering Performance of Lifting Reentry Vehicles," ARS Journal, March 1962, pp. 346-354.

4. Shaver, R. D., Minimum Energy Loss Heading Changes for Hypersonic Flight from Orbit, The RAND Corporation, RM-4391-PR, December 1964.

5. Nyland, F. S., The Synergetic Plane Change for Orbiting Spacecraft, The RAND Corporation, RM-3231-PR, September 1963; also in the Proc. 5th International Symposium on Space Technology, Tokyo, 1963.

6. Williams, E. P., et al., Long Range Surface-to-surface Rocket and Ramjet Missiles - Aerodynamics, The RAND Corporation, R-181, May 1, 1950, 2nd Printing, April 1959.

7. Gazley, Carl, Jr., Atmospheric Entry, The RAND Corporation, P-2052, July 15, 1960.

8. Jahnke, Eugene, and Fritz Emde, Tables of Functions with Formulae and Curves, Dover Publications, New York, 1945.

9. Loh, W. H. T., A Second Order Theory of Entry Mechanics into a Planetary Atmosphere, Chance Vought Research Center, Report No. RE-IR-11, 18 May 1961, Dallas, Texas.